Polymer Testing 94 (2021) 107002

Contents lists available at ScienceDirect

Polymer Testing

journal homepage: http://www.elsevier.com/locate/polytest

A phenomenological criterion for an optical assessment of PE-HD fracture surfaces obtained from FNCT

Markus Schilling [a], Ute Niebergall [a], Niklas Marschall [a], Ingo Alig [b], Martin Böhning [a,*]

[a] Bundesanstalt für Materialforschung und –prüfung (BAM), Unter den Eichen 87, 12205, Berlin, Germany
[b] Bereich Kunststoffe, Fraunhofer-Institut für Betriebsfestigkeit und Systemzuverlässigkeit LBF, Schlossgartenstraße 6, 64289 Darmstadt, Germany

ARTICLE INFO

Keywords:
Environmental stress cracking (ESC)
Full notch creep test (FNCT)
Laser scanning microscopy (LSM)
Fracture surfaces
Optical criterion of brittleness

ABSTRACT

The full-notch creep test (FNCT) is a common test method to evaluate the environmental stress cracking (ESC) behavior of high-density polyethylene (PE-HD), e.g. for container materials. The test procedure as specified in ISO 16770 provides a comparative measure of the resistance against ESC using the time to failure of PE-HD specimens under constant mechanical load in a well-defined liquid test environment. Since the craze-crack damage mechanism underlying the ESC phenomenon is associated with brittle failure, the occurrence of a predominantly brittle fracture surface is a prerequisite to consider an FNCT measurement as representative for ESC, i.e. a time to failure dominated by craze-crack propagation.

The craze-crack propagation continuously reduces the effective residual cross-sectional area of the specimen during the test, which results in a corresponding increase of the effective mechanical stress. Thus, a transition to ductile shear deformation is inevitable at later stages of the test, leading usually to a pronounced central ligament.

Therefore, an optical evaluation of FNCT fracture surfaces concerning their brittleness is essential. An enhanced imaging analysis of FNCT fracture surfaces enables a detailed assessment of craze-crack propagation during ESC. In this study, laser scanning microscopy (LSM) was employed to evaluate whether FNCT fracture surfaces are representative with respect to craze-crack propagation and ESC. Based on LSM height data, a phenomenological criterion is proposed to assess the validity of distinct FNCT measurements. This criterion is supposed to facilitate a quick evaluation of FNCT results in practical routine testing. Its applicability is verified on a sample basis for seven different commercial PE-HD container materials.

1. Introduction

The well-known damage mechanism environmental stress cracking (ESC) is essentially a failure due to slow crack growth (SCG) [1–5] strongly accelerated by presence of certain fluids. Both closely related phenomena, SCG and ESC, are considered major failure modes of high-density polyethylene (PE-HD) parts and components [6]. Generally, PE-HD is used in several high-performance applications, predominantly as materials for pipes but also for geosynthetic barriers as well as packaging material, i.e. for jerrycans, drums and intermediate bulk containers (IBC) [7]. Especially when these are used for storage and transport of various dangerous liquids, the resistance against ESC becomes a highly safety relevant issue. Therefore, meaningful test procedures addressing SCG and ESC phenomena and the resistance of PE materials against them are essential. In this work, the so-called Full Notch Creep Test (FNCT) is considered which is widely used (especially in Europe) to test PE-HD materials with respect to their resistance against environmental stress cracking (ESCR) [8,9].

Typically, a crack emerges due to a pre-existing defect in the polymer material and crack propagation occurs at stress levels well below the yield strength of the polymer [1,5]. The underlying craze-crack mechanism can be used to identify SCG and ESC and distinguish them from other modes of failure because it leads to the intermediate formation of fibrils that leaves behind a characteristic fracture surface. This is actually the starting point of this work, since the FNCT only represents ESC or SCG behavior if craze-crack propagation is the dominating damage mechanism leading to failure of the test specimen and determining the observed time to failure - the antagonistic mechanism is usually ductile shear deformation. This time to failure obtained under well-defined and standardized conditions in a certain liquid is then taken as a measure to

* Corresponding author.
E-mail addresses: Ingo.Alig@lbf.fraunhofer.de (I. Alig), martin.boehning@bam.de (M. Böhning).

https://doi.org/10.1016/j.polymertesting.2020.107002
Received 19 June 2020; Received in revised form 11 November 2020; Accepted 1 December 2020
Available online 7 December 2020

characterize the intrinsic resistance of PE-HD materials. On the other hand, the aggressiveness of different media can also be addressed. In both cases the dominance of the craze-crack mechanism has to be verified for every single test.

For PE-HD, crack propagation due to SCG as well as ESC results from a craze-crack mechanism initiated at a local stress concentration, typically due to a tiny defect or a scratch in the polymer material. First, microvoids are persistently developing in the zone of plastic deformation at the forefront of the preformed crack tip. In the course of progressing growth and opening of the crack, highly orientated polymer fibrils are formed from the material in between these voids, designated as crazes. Crack propagation occurs when the fibrils in the craze zone start to fail by either chain scission or disentanglement [2]. As the phenomenon takes place at a local stress peak at the crack tip, the overall mechanical stress may be quite low. At higher overall stresses, a transition to shear deformation across the entire remaining cross-sectional area occurs.

Failure of the microscopic fibrils in the course of craze-crack propagation results in a characteristic globally brittle fracture surface [1,10,11], which is especially to be distinguished from globally ductile fracture surfaces originating from shear deformation [12–15]. It should be noted that such a globally brittle fracture surface actually appears ductile when investigated on a sub-micrometer scale (e.g. with SEM). As the local stress in terms of a single fibril is quite high, the failure of individual microscopic fibrils is ductile showing a typical tapered extension. This results microscopically in a characteristic lawn-like surface structure [1,16,17] which nevertheless appears brittle on a macroscopic scale of about 100 μm.

In practical tests for the assessment of PE-HD materials with regard to their ESC resistance, specimens and conditions have to be selected in a way that leads to such globally brittle fracture surfaces, indicating that craze-crack propagation was the dominating process determining the time-to failure in order to consider the test as representative for ESC. In this respect, the initial stress applied to a specimen is the crucial factor. The FNCT is performed under constant load on the specimen, i.e. under constant force representing the initial stress with respect to the initial cross-sectional area. In the course of the test, the progressing crack continuously reduces the effective residual cross-sectional area which implies that inevitably, the effective stress is increasing and at a certain point exceeds the threshold to overall ductile behavior. Accordingly, the very last stages of the test are always ductile in nature [12,18]. This usually results in the formation of a larger central ligament. Hence, the failure mechanism can never be assigned to craze-crack propagation exclusively, but it rather has to be ensured that this is the dominating mechanism determining the observed time to failure.

Furthermore, the FNCT, as most other related test methods, includes the application of a well-defined notch in the specimen for crack initiation to focus on craze-crack propagation by ESC. This provoked crack initiation also reduces overall test durations to practically feasible timescales. A constant mechanical load impinged on the specimens results in progressive crack growth during the test due to craze-crack propagation and finally leads to characteristic failure [5,10,19]. The time to failure t_f obtained from the test under pre-defined conditions (specimen geometry, mechanical stress, temperature and test liquid) is taken as a relative measure of the resistance against ESC.

The full-notch creep test (FNCT) is specified in ISO 16770 [19]. The standard quotes an aqueous solution of a neutral surfactant (e.g. Arkopal N100) as liquid environment for the test. The corresponding geometry of FNCT specimens ensures plane strain conditions as encountered in most practical applications [20]. The tensile load and test temperature are to be selected appropriately to obtain valid ESC conditions. The standard test procedure requires a simple optical check of the fracture surface to ensure brittle behavior and a microscopic measurement of notch depth and actual initial ligament area for calculation of the actual applied stress. However, the simple classification of FNCT fracture surfaces given in ISO 16770 based on an optical assessment by the naked eye is sometimes ambiguous, subjective and thus remains unsatisfactory.

Table 1
Investigated PE-HD types; density and melt flow rate data were obtained from data sheets of the respective producers.

PE-HD type	density/g cm^{-3}	Melt flow rate (MFR)/g $10min^{-1}$
PE-HD 1	0.945[a]	6.0[c]
PE-HD 2	0.949[a]	7.0[c]
PE-HD 3	0.949[b]	7.0[c]
PE-HD 4	0.949[a]	7.0[c]
PE-HD 5	0.945[b]	6.2[d]
PE-HD 6	0.950[a]	22.0[c]; 0.25[e]
PE-HD 7	0.959[b]	0.35[e]

Note: The determination of the melt flow rate (MFR) in accordance with the test conditions in [3] and [4] is similar. Therefore, the corresponding MFR values are directly comparable. Furthermore, MFR values of PE-HD 6 were quoted for both test conditions given in [3] and [5] to enable a direct comparison to the MFR values of PE-HD 1 to 5 and of PE-HD 7. Accordingly, the MFR values of PE-HD 6 and 7 are in the same range and distinctly higher than the values of PE-HD 1 to 5.

[a] Density determined according to ISO 1183.
[b] Density determined according to ASTM D 1505.
[c] MFR determined according to ISO 1133 at 190 °C/21.6 kg.
[d] MFR determined according to ASTM D 1238 at 190 °C/21.6 kg.
[e] MFR determined according to ASTM D 1238 at 190 °C/2.16 kg.

Based on earlier work on the FNCT concerning the transition from brittle to ductile behavior and a detailed analysis of fracture surfaces using laser scanning microscopy (LSM) [2,18], a first attempt for an objective criterion derived from measured quantitative height-profile data is presented. This may be used in practical tests for a reliable differentiation of brittle and ductile fracture surfaces to confirm the validity of single FNCT experiments with respect to ESC or SCG.

An independent method for the differentiation between the two failure modes, craze-crack propagation (brittle) and shear deformation (ductile), is based on the results of a series of FNCT measurements with varying the nominal initial stress. Therein, two linear regions are observed in the obtained curve of actual initial stress σ_L vs. time to failure t_f in a double-logarithmic plot, representing ductile failure at higher stresses and brittle behavior at lower stresses [19]. The dependence of the observed time to failure on the stress changes distinctly. Hence, FNCT experiments addressing ESC are to be performed at nominal stresses from the lower branch region.

Some orientation in this respect is given by Qian et al. who state that predominantly ductile failure results as soon as the external stress becomes much higher than about one-half of the yield strength of the PE-HD material [15]. At that point, the brittle-ductile transition from the craze-crack to the shear deformation mechanism occurs. Therefore, the application of stresses lower than half of the yield strength is recommended. In another practical approach, a minimum of 30% of the fracture surface to be brittle is simply suggested as empirical criterion for considering an FNCT experiment as valid [21].

This somewhat unsatisfactory situation makes an objective measurement-based criterion for the differentiation between predominantly brittle and predominantly ductile failure most welcome.

It was found in our previous work that the characteristic features of FNCT fracture surfaces, which may be considered for this differentiation, vary distinctly for different PE-HD materials [18] and therefore, a corresponding criterion might not be derived straightforward.

Our approach comprises the investigation of seven PE-HD materials - typically used for containers for storage and transport of dangerous goods - using the FNCT with a detailed fracture surface analysis based on micrographs and height data obtained by laser scanning microscopy (LSM). The three-dimensional representations of the fracture surfaces shown in this study are consistent with images in our previous publications [2,18] with respect to height color-coding and resolution. The LSM provides height profile data of FNCT fracture surfaces with a resolution in the sub micrometer region which not only enables their depiction as three-dimensional images but also a quantitative analysis

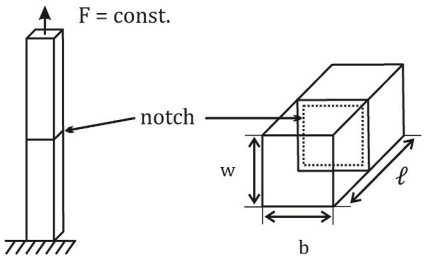

Fig. 1. Schematic representation of the FNCT specimen geometry (ℓ = 90 mm, w = b = 6 mm) according to specimen C in ISO 16770 [19].

concerning distinct fracture surface features on different length-scales.

This technique is combined with the systematic variation of the initial stress for the FNCT which allows the unambiguous identification of brittle and ductile behavior (discussed above).

2. Materials and test liquid

2.1. PE-HD types

A total of 7 typical PE resins (PE-HD types) commercially available and practically relevant in the field of container applications were selected for this study (Table 1).

The investigated PE-HD types cover a broad range of high-performance container applications from small blow molding products such as bottles and consumer goods (PE-HD 6 and 7) to packaging of dangerous goods in intermediate bulk containers (IBC), heating oil tanks (HOT) and agricultural containers (PE-HD 1 to 5). Taking additional account of their stabilizer packages, they are supposed to exhibit not only good ESC resistance but also good processability and long-term durability. The PE-HD resins were kindly provided by several internationally active PE-HD manufacturers.

2.2. Test liquid

The liquid used for all tests in this study is based on the standard FNCT procedure for common PE-HD types described in ISO 16770. A 2 wt% aqueous solution of a neutral-type 4-nonylphenoxy-(ethyleneoxy)-ethanol with an average molecular weight of 680 g/mol, Arkopal N 100, was used. Arkopal N 100 was kindly provided by Clariant GmbH, Frankfurt/Main, Germany. To ensure comparable results, the solution was aged for 14 days at the test temperature of 50 °C as also specified in ISO 16770.

Sorption measurements confirmed that the mass uptake by the specimens is negligible (see Supplementary data, Fig. S1).

2.3. Sample preparation

Specimens for FNCT and subsequent LSM analysis were cut according to type C in ISO 16770 with dimensions of (90 × 6 x 6) mm^3 (Fig. 1) from sheets of 6 mm thickness. The latter were prepared in a heated press under conditions according to ISO 293 [22] and ISO 17855 [23], i. e. for 5 min at a press temperature of 180 °C and a pressure of 10 MPa. The cooling rate was about 15 K/min and sheets were removed below 40 °C. In an additional step, they were subsequently annealed for 3 h at 100 °C. FNCT specimens were circumferentially notched (depth = 1 mm) using a semiautomatic notching device, which meets the requirements of ISO 16770 [19], ISO 13274 [24] and ISO 11542 [25].

3. Experimental

3.1. FNCT procedure

An advanced FNCT device of IPT (Institut für Prüftechnik Gerätebau,

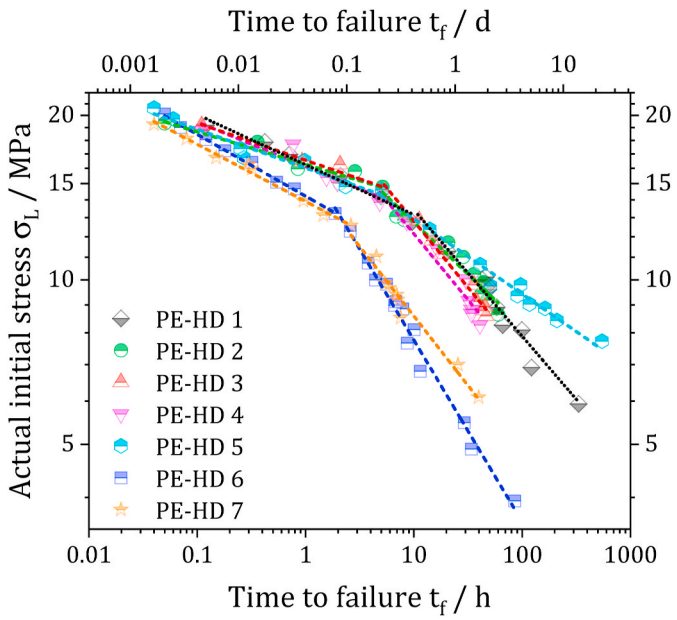

Fig. 2. FNCT t_f tested at 50 °C in a 2 wt% aqueous solution of Arkopal N 100 over a large range of actual initial stresses σ_L (in accordance with ISO 16770 [19]).

Todtenweis, Germany) was employed to obtain FNCT results as well as to produce samples for further LSM analysis (section 3.2). In addition to the time to failure t_f, this FNCT device continuously records the time-dependent elongation of specimens. Each specimen is clamped for testing in a separate stainless-steel cylinder containing the continuously stirred and temperature-controlled test liquid. A constant force is applied (Fig. 1) and maintained by a stepping motor combined with a stress gauge. A heating plate under each individual test cylinder sets the test temperature. A more detailed description of the FNCT device can be found in Ref. [18,26].

The standard procedure according to ISO 16770 comprises a conditioning of clamped specimens in the temperature-controlled test fluid for 10 h prior to applying the nominal load. The test temperature and the nominal initial mechanical stress σ_n are defined to be 50 °C and 9 MPa, respectively, for typical PE-HD container materials. These test parameters are supposed to provide conditions that lead to brittle fracture of most PE-HD types.

However, nominal initial stress values were varied in this study to deliberately produce predominantly brittle as well as ductile FNCT fracture surfaces. Especially, the PE-HD type dependent development of distinct fracture surface features such as typical central ligaments were assessed with respect to an evaluative criterion.

Furthermore, the actual notch depth and the actual initial residual cross-sectional area (ligament area A_L after notching) were determined precisely after each FNCT by light microscopy (LM) in order to calculate the actual initial stress σ_L for each specimen (Eq. (1)):

$$\sigma_L = \frac{F}{A_L} \tag{1}$$

Accordingly, every analyzed fracture surface can be assigned to the initial stress value the regarded specimen was actually tested with.

In this study, FNCT experiments were performed at 50 °C in a 2 wt% aqueous solution of Arkopal N 100 (according to the standard conditions given in ISO 16770). To ensure a reproducible starting point of the measurement, the application of a moderate pre-load is inevitable. It is applied smoothly with a rate of 1 N/s just before the measurement. The continuous recording of the elongation starts immediately after reaching the pre-load, which is typically in the range of 30 N. The force used for the measurement is in the range of 150 N for the selected specimen

geometry.

First, the time-to failure for the nominal load of 9 MPa was determined by a series of five individual measurements with load levels varying around the nominal value of 9 MPa (usually 8.25, 8.75, 9.0, 9.25, and 9.75 MPa). The determination of the nominal time to failure t_f^* is then performed by interpolation to the exact nominal stress value using a linear regression in a double-logarithmic plot of individual values t_f vs. the actual stress σ_L.

In contrast to that, the extended series of stress-variation data points with significantly higher or lower initial stress were obtained by single FNCT measurements. All data points were used to obtain the double-logarithmic plot of t_f vs. σ_L (see Fig. 2) which allows the identification of the transition between brittle and ductile behavior for all PE-HD types under investigation. At the same time, the specimens (after failure) provided the fracture surfaces for the subsequent analysis.

3.2. Fracture surface analysis by light microscopy (LM) and laser scanning microscopy (LSM)

Light microscopy (LM) (AxioCam ICc 3 on a Stemi 2000-C microscope, Carl Zeiss AG, Oberkochen, Germany) was only performed to determine the initial residual cross-sectional area of each individual specimen to subsequently calculate the actual initial stress applied σ_L during FNCT measurements (cf. section 3.1).

A more detailed fracture surface analysis especially concerning distinct surface features was achieved by laser scanning microscopy (LSM) using a VK-X 100 of Keyence GmbH, Neu-Isenburg (Germany), which is equipped with a semiconductor laser (wavelength of 658 nm). Besides detailed height information of the investigated fracture surfaces, the LSM procedure provides a high-contrast achromatic (65536 gray shades) laser picture. Laser scans were performed with a window of (2048 × 1536) pixels and a height resolution of 5 nm. To cover the larger height range of practical relevance, multiple scans were performed with a height-increment of 12 µm, respectively. From these LSM height information, expressive three-dimensional images of FNCT fracture surfaces were obtained.

For alignment reasons (the notch plane of the specimen defines the zero height level) and to apply appropriate consistent scaling of the height information (z-axis), 3D-data of the fracture surfaces were transferred to the graphing and data analysis software Origin (OriginLab Corporation, Northampton, MA, USA). An average height value was calculated for each fracture surface, which is based on height values of 500 by 100 data points measured in the circumferential notch area and set as height value defining the zero level. After zero-level shifting of all data points (subtracting the average height value, respectively), pixel-based data were transformed to metric data and gridded using the Renka-Cline interpolation method [27] (as implemented in Origin). Subsequently, data was plotted as a color-coded 3D surface image. Height data in these plots are represented with reference to a z-axis up to 3 mm. The color coding of the height data was applied in the range of -0.10 mm to +0.18 mm which allows for a detailed identification of smaller surface features. Height values > 0.18 mm are uniformly colored in brown, those < - 0.1 mm in black. This scheme was also used for the LSM fracture surfaces previously presented in Ref. [2,18].

4. Results and discussion

The change of fracture characteristics of FNCT specimens investigated with respect to ESC, i.e. the balance of brittle and ductile fracture, with increased stress or temperature is well known [18]. These changes become visible most prominently on the fracture surface which, in turn, can be used to identify the respective proportions and to evaluate the significance of results with regard to ESC resistance [2,10,11,18,19]. Up to now, this is done by the naked eye. Taking into account that features of fracture surfaces of different types of PE-HD also differ in their distinctiveness [18], the approach presented is based on quantitative

Table 2
Data of typical failure times t_f^* corresponding to the nominal initial stress σ_n of 9.00 MPa and transition regions from brittle to ductile fracture behavior.

PE-HD type	t_f^* related to σ_n = 9.00 MPa /h	brittle/ductile transition point /MPa
PE-HD 1	56.6	13.1
PE-HD 2	52.8	14.9
PE-HD 3	42.1	14.7
PE-HD 4	40.9	14.1
PE-HD 5	158.4	14.3
PE-HD 6	6.7	13.2
PE-HD 7	8.0	12.5

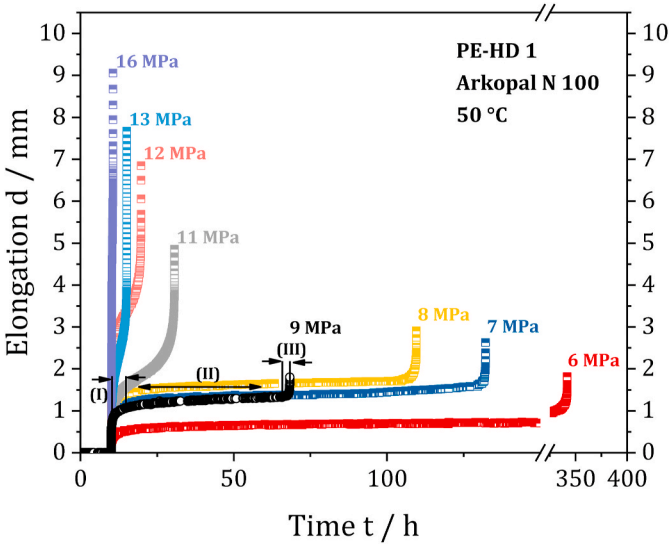

Fig. 3. Time-dependent elongation curves representing the progressing damage of PE-HD 1 for various initial stresses.

height data considering features on different length scales. Data were obtained from LSM analysis of fracture surfaces applying a systematic variation of the initial stress in FNCT experiments performed in an aqueous Arkopal N 100 solution at 50 °C.

4.1. Brittle-ductile transition from typical stress/time-to- failure plot

First, the nominal time to failure (50 °C, 9.00 MPa) was determined for all PE-HD materials under investigation based on the five-point-interpolation described above. Then, the linear regions of brittle and ductile behavior at 50 °C as well as the transition between the two were identified by an extended series of stress-variation. Results are shown in Fig. 2 and summarized in Table 2. The approximate transition point given in Table 2 should be regarded as the estimated center of the expected transition region.

For all PE-HD types examined in this study, a typical curve of actual initial stress σ_L vs. failure time t_f is obtained (Fig. 2). All curves exhibit a distinct 'knee' (kink), which represents the transition region from predominantly brittle to ductile fracture behavior.

From the curves of σ_L vs. t_f as well as from the data of t_f^* related to σ_n = 9.00 MPa, two different groups of PE-HD types can be recognized: group A comprises the PE-HD types 1 to 5, which exhibit higher t_f^* (Tab. 2) and the curves in Fig. 2 are located at higher σ_L and t_f. The PE-HD types 6 and 7, which form group B, show rather low t_f^*. These differences might have been expected since the PE-HD types in group A are designed and used for high-performance applications such as IBC manufactured by blow-molding, whereas group B comprises PE-HD types also suitable for injection molding (section 2.1). This is indicated by the distinctly different melt flow rates (MFR, see Table 1) which correspond

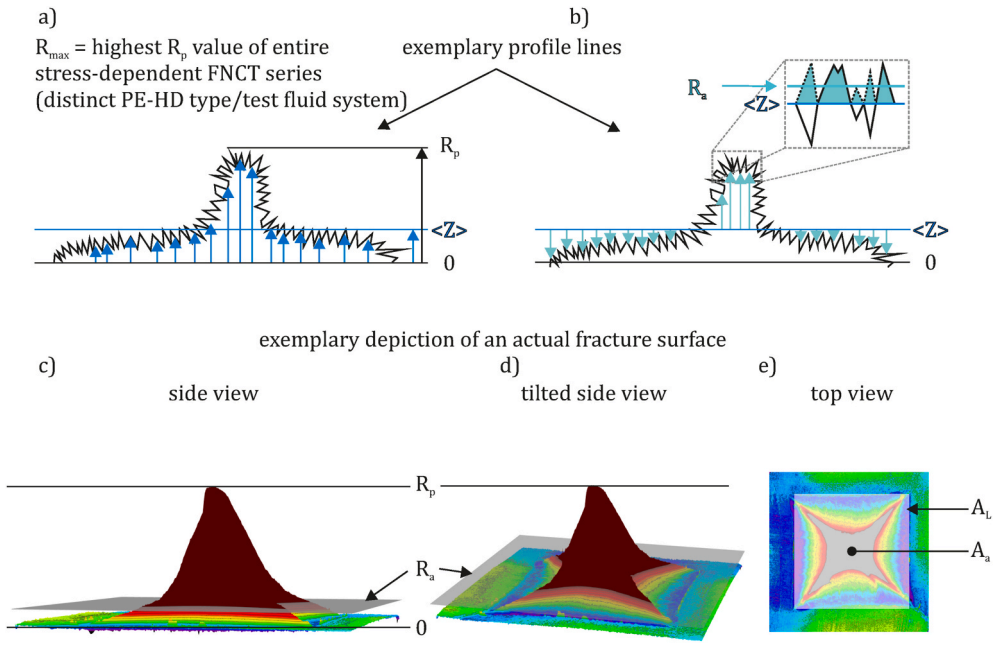

Fig. 4. Schematic depiction of parameters used in the criterion of brittleness B, a) exemplary profile line with R_p, R_{max} and ⟨Z⟩, b) exemplary profile line with R_a and ⟨Z⟩, c), d), e) exemplary depictions of an actual fracture surface (ductile) with R_p, R_a, A_L and A_a.

to the application/processing properties but are also related to those fundamental molecular characteristics which affect the ESC resistance.

The transition regions from predominantly brittle to ductile fracture behavior for all PE-HD types are generally in a range from approx. 12.5 MPa to approx. 14.9 MPa, with group A around 14.5 MPa (PE-HD1 being at about 13.1 MPa) and group B around 13 MPa, again reflecting the characteristics mentioned above.

The FNCT device employed in this study enables monitoring of the effective elongation of the specimen which allows to follow the time-dependent course of the FNCT experiment (section 3.1). The effect of the applied stress on the time-dependent behavior and consequently, on shear deformation vs. crack propagation can be seen in Fig. 3, in which the time-dependent elongation of the FNCT specimens (PE-HD 1) is depicted. As indicated exemplary for the 9 MPa (initial stress) curve, the almost linear section (II) of the elongation curve represents the major part of crack propagation, whereas section (I) is assigned to immediate orientational and relaxational processes as well as initial craze formation, and section (III) clearly corresponds to ductile shear deformation and final failure (break) [18].

In the stress-range above 12 MPa, section (II) indicating crack propagation no longer dominates the overall time to failure but quickly vanishes completely (see also Fig. S2 in the Supplementary data). This is in agreement with the location of the transition region in Fig. 2. Furthermore, the ductile behavior above 12 MPa also results in significantly higher elongation values corresponding to the formation of a massive central ligament.

4.2. Criterion of brittleness B in FNCT

Inspired by the usual distinction between brittle and ductile fracture surfaces to assess the validity of an FNCT (according to Ref. [19]), a criterion of brittleness B is proposed that is based on results obtained from LSM fracture surface analysis. As detailed in this section, surface roughness parameters, heights of distinct surface features and proportions of surface areas are therefor considered.

Two parameters are supposed to be decisive for the assessment of an FNCT fracture surface in terms of brittleness: (1) the overall height of the highest surface peak (typically the central ligament) and (2) its area. Simply put, a fracture surface will be denoted as ductile, if (1) or (2) or both adopt high values.

The peak area is defined as the surface fraction A_a which is higher than the overall surface roughness R_a, which is obtained by considering the entire fracture surface A_L.

From an earlier investigation comparing two PE-HD materials with distinctly different MFR, it is known that the overall structure and the height of local features of the fracture surface can differ significantly [18], i.e. some PE-HD types tend to form high central ligaments, while others inherently show rather flat fracture surfaces. Therefore, the starting point of this approach is the consideration of the height of the highest peak (typically the central ligament) and the variation of the average height of the entire fracture surface determined as surface roughness R_a, both relative to the zero-level defined by the notch-plane of the specimen. R_a is determined according to Eq. (2) and Eq. (3) considering the arithmetic average of the height profile <Z> of the entire fracture surface [28]:

$$R_a = \frac{1}{MN}\sum_{m=1}^{M}\sum_{n=1}^{N}|Z(x_m, y_n) - \langle Z\rangle| \tag{2}$$

with

$$\langle Z\rangle = \frac{1}{MN}\sum_{m=1}^{M}\sum_{n=1}^{N}Z(x_m, y_n) \tag{3}$$

and $Z(x_m, y_n)$: height value of a pixel on the fracture surface and ⟨Z⟩: mean of height values of all pixels on the fracture surface.

It is now possible to define the area of the central ligament A_a (Fig. 4e) as the area which is higher than the roughness R_a of the entire fracture surface area (Fig. 4c–e). This allows the determination of the proportion of the area of the central ligament A_a - which represents a ductile fraction in any case - in relation to the entire fracture surface A_L.

Considering the limiting cases derived from the fracture surfaces obtained in this study, it becomes obvious that the area A_a is not sufficient for a reliable differentiation of the overall failure mechanism between brittle craze-crack growth and ductile shear deformation. The height of the central ligament has to be taken into account as well. The highest peak on a particular fracture surface (height profile) under investigation is denoted R_p, whereas the highest peak among all fracture

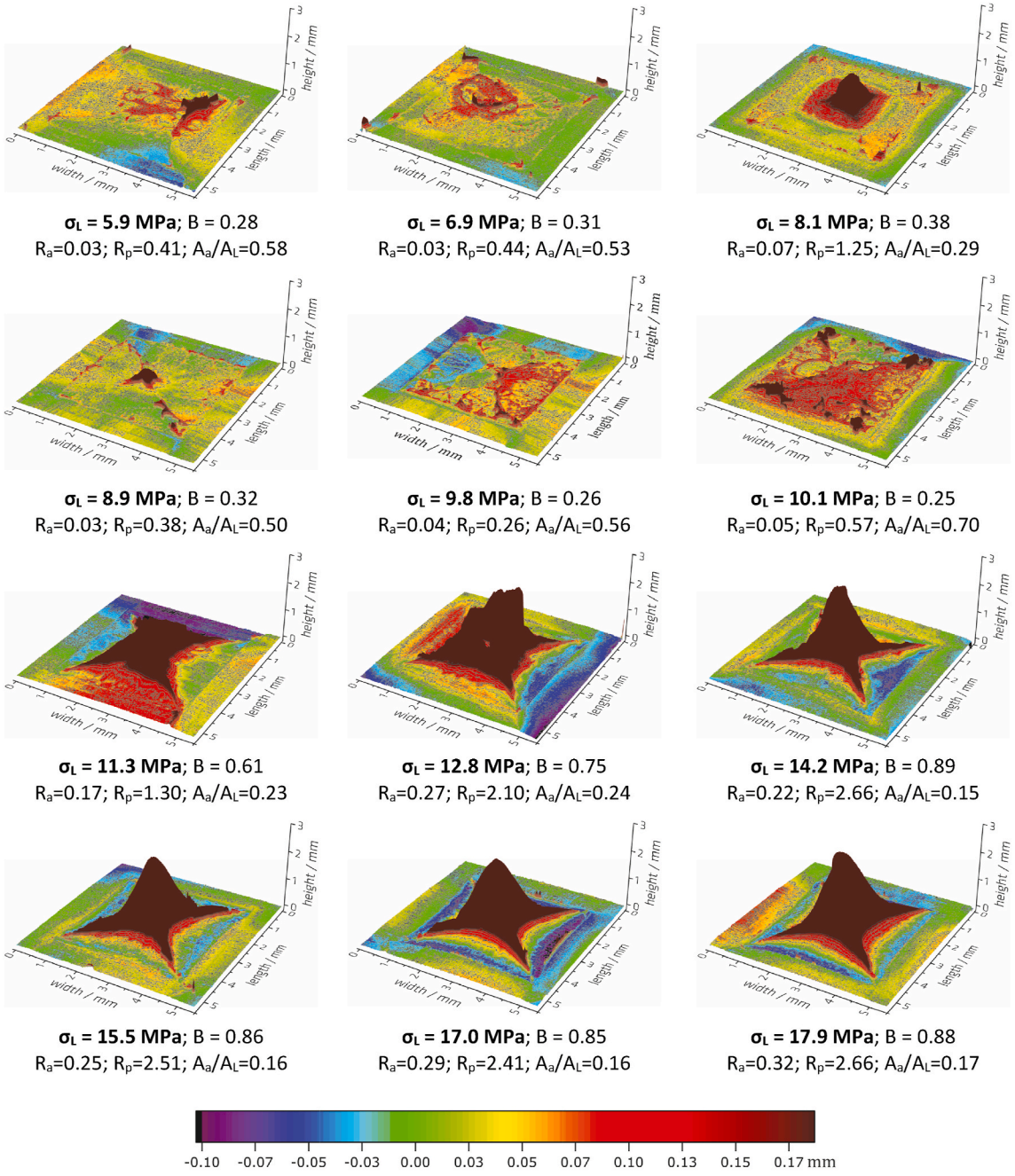

Fig. 5. Series of fracture surfaces obtained by LSM for PE-HD 1 (50 °C in Arkopal) at increasing initial stress together with the respective parameters B, R_a/mm, R_p/mm and A_a/A_L.

surfaces in a stress dependent FNCT series (in a certain test fluid), i.e. the highest possible peak, is denoted R_{max}.

Hence, the criterion of brittleness, denoted B, comprises the two parameters:

$\frac{R_p}{R_{max}}$ and $\frac{A_a}{A_L}$,

R_p: maximum height of fracture surface (profile).

R_{max}: maximum height of all fracture surfaces in a stress-dependent FNCT series of the distinct PE-HD type-test fluid system.

A_L: actual initial cross-sectional area after notching (section 3.1).

A_a: area on the fracture surface overtopping R_a (number of pixels having height value $Z > R_a$, Fig. 4 *c*-e).

To follow this approach, the highest possible peak value characteristic for a specific combination of PE-HD type and test fluid should be obtained from a stress-dependent FNCT series first.

An FNCT fracture surface is considered predominantly brittle and thus valid for evaluation in terms of craze-crack propagation, if characteristic surface features (e.g. the central ligament) are small and the surface roughness is low. This is represented by $\frac{R_p}{R_{max}} < 0.5$ and $\frac{A_a}{A_L} > 0.5$. Accordingly, the criterion of brittleness B, based on empirical fracture surface data, is defined as (Eq. (4)):

$$B = \frac{1}{2}\left[\frac{R_p}{R_{max}} + \left(1 - \frac{A_a}{A_L}\right)\right] \quad (4)$$

with $B < 0.5$ characterizing a brittle, valid and $B > 0.5$ indicating a ductile, invalid fracture surface. Thus, both terms are weighed equally as an obvious first assumption.

The edge case of $B = 0.5$ only occurs for FNCT specimens without

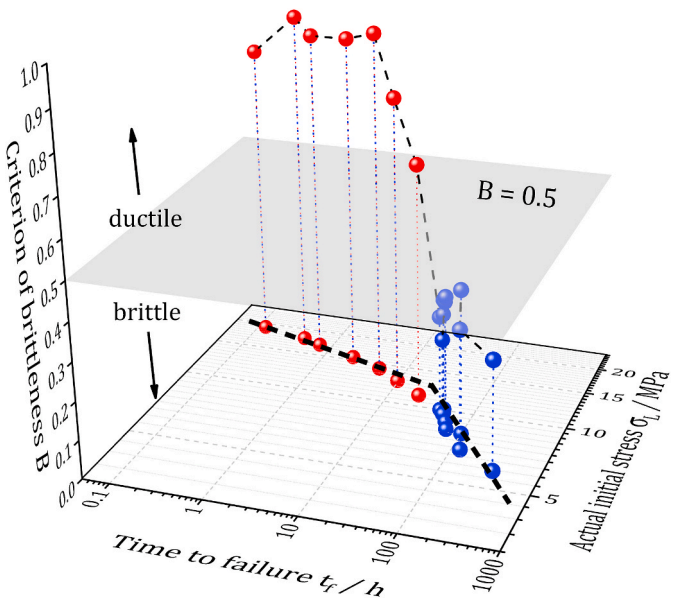

Fig. 6. Criterion of brittleness B vs. time to failure t_f and actual initial stress σ_L, exemplary for PE-HD 1.

crack propagation, since the parameters $\frac{R_p}{R_{max}}$ and $\frac{A_a}{A_L}$ would have to adopt the same values. This would only be possible when R_p equals R_{max} and the entire surface area is concurrently higher than R_a. In such a case, there would be no crack propagation and the fracture surface would consequently be non-evaluable. Moreover, $\frac{R_p}{R_{max}}$ and $\frac{A_a}{A_L}$ influence each other, since R_p is included in R_a. Therefore, they are self-regulating and contradictions resulting from their individual consideration are prevented. Furthermore, differences in the characteristic fracture surface appearances between different PE-HD types are accounted for: either an increased overall height (R_p) or a high surface roughness (R_a, A_a) predominantly contributes to the determination of B (Eq. (4)).

It is expected that for stress- or temperature-dependent experiments, a transition region rather than a transition point between brittle and ductile fracture behavior (see Fig. 2) may be determined using the criterion B. As a first estimation of the uncertainty of this approach, the deviation between the two fracture surfaces for one specimen is considered. A comparison was performed for five specimens with a brittle fracture surface (cf. Fig. S3 in the Supplementary data). In the calculation of B, the surface roughness and the ligament height have the main influence and from the pythagorean addition of their uncertainties, the uncertainty for the criterion is estimated as 10%. Based on empirical experience and the analysis of uncertainties and their propagation, the range of $0.45 < B < 0.55$ is considered as transition region. Fracture surfaces leading to B values within this range must be regarded with due care since they might be part of this brittle/ductile transition region.

All results obtained within the framework of this study are mapped in a plot $\frac{R_p}{R_{max}}$ vs. $\left(1-\frac{A_a}{A_L}\right)$ (Fig. S4 in the Supporting Information), also showing the threshold and transition region of B. Moreover, this plot demonstrates that just one of the two terms included in B would not be sufficient for the intended distinction between brittle and ductile fracture behavior.

It has to be noted, that in the unlikely case of a non-uniform fracture of an FNCT specimen with respect to the ligament lengths on both fracture sides, i.e. if the features (e.g. the central ligament) differ significantly between both fracture parts, the fracture side with the more pronounced fracture features (higher values of R_p and R_a) should be considered within the calculation of B. With this consideration of the more ductile fracture side, a questionable fracture surface is rather rejected.

The development of B with increasing initial stress is illustrated exemplary for PE-HD 1 in Fig. 5.

To show the agreement of the results with respect to the distinction of brittle and ductile fracture behavior, the correlation of the criterion of brittleness B and the actual stress applied vs. time to failure obtained from the classic analysis (cf. Fig. 2) is depicted in Fig. 6 exemplary for PE-HD 1.

The fracture surfaces of specimens assigned to the lower branch in the actual stress vs. time to failure graph result in B values lower than 0.5 indicating brittle fracture behavior (blue dots in Fig. 6). Accordingly, the specimens represented by red dots in Fig. 6 showed ductile fracture behavior, which is revealed by $B > 0.5$. Their time to failure values furthermore range in the upper branch in the actual stress vs. time to failure curve, which also corresponds to ductile fracture behavior.

In Figs. 7 and 8, fracture surfaces of different PE-HD types are compared for B values within the brittle region (i.e. valid FNCT with dominating craze-crack propagation), the transition region and the ductile region (with dominating shear deformation, not evaluable with regard to SCG or ESC). Fracture surfaces of the region of brittle/ductile transition are obtained from FNCT experiments within the respective region identified by the plots of the actual initial stress σ_L vs. the corresponding failure time t_f (Fig. 2).

In this study, LSM data and an analysis procedure employing Origin software (section 3.2) were used subsequent to extensive FNCT experiments to obtain B values. Fundamentally, a variety of methods arbitrarily selected and easy to perform may be applied to calculate B, as long as the required parameters (R_p, R_a, R_{max}) are obtained in acceptable accuracy. The determination of R_{max} basically requires the performance of an entire stress-dependent FNCT series of a distinct system of PE-HD type and test fluid. Since the maximum height of fracture surface features usually correlates to the initial stress applied in FNCT [18], a measurement of fracture surface features from a single test at a high initial stress might be sufficient (e.g. FNCT at 18 MPa for PE-HD 1 in this study). Once determined, R_{max} is valid for the regarded system of PE-HD type and test fluid. Therefore, R_{max} could be used for all upcoming measurements and subsequent calculation of B in quality control processes and would not have to be determined repeatedly.

Applying the criterion of brittleness B, FNCT fracture surfaces of seven different PE-HD types could reliably be assessed in terms of their evaluability concerning ESC by assigning them to predominantly brittle or ductile fracture behavior, respectively (Figs. 7 and 8). Hence, B is a valuable tool to evaluate the brittle/ductile transition region and FNCT validity of PE-HD container materials.

The grouping of PE-HD types also noted in the data of actual initial stress σ_L vs. failure time t_f is recurred in the appearance of FNCT fracture surfaces: The predominantly brittle as well as the predominantly ductile fracture surfaces differ significantly between group A (PE-HD 1 to 5) and group B (PE-HD 6 and 7). For the PE-HD types in group A, more prominent and extended ligaments are formed, whereas the structures of the fracture surfaces of PE-HD types in group B are flatter and appear more brittle in general. This can also be read from the different R_{max} values, which are much lower for the PE-HD types in group B. This seems plausible, since R_{max} is a measure for the basic ability of a PE-HD type to form ligaments and describes their manifestation. In this respect, a relation between R_{max} and the MFR of a distinct PE-HD type is reasonable, which can also be seen from the data in this study:

Both differ decisively between groups A (MFR around 7 g/10min) and B (MFR > 20 g/10min) (Table 1, Figs. 7 and 8). Since the MFR correlates to the toughness determined by Charpy impact tests [29], it might also represent an indicator of pronounced fracture surface features resulting from FNCT. A high MFR represents a low viscosity and a low (Charpy) toughness. Accordingly, a low MFR indicates a high ductility and prominent FNCT fracture surface features, such as in group A compared to group B. This is plausible, since the MFR is a technical parameter which is determined by viscosity. The viscosity of a polymer is a measure of its flowability, and it is affected by the structural

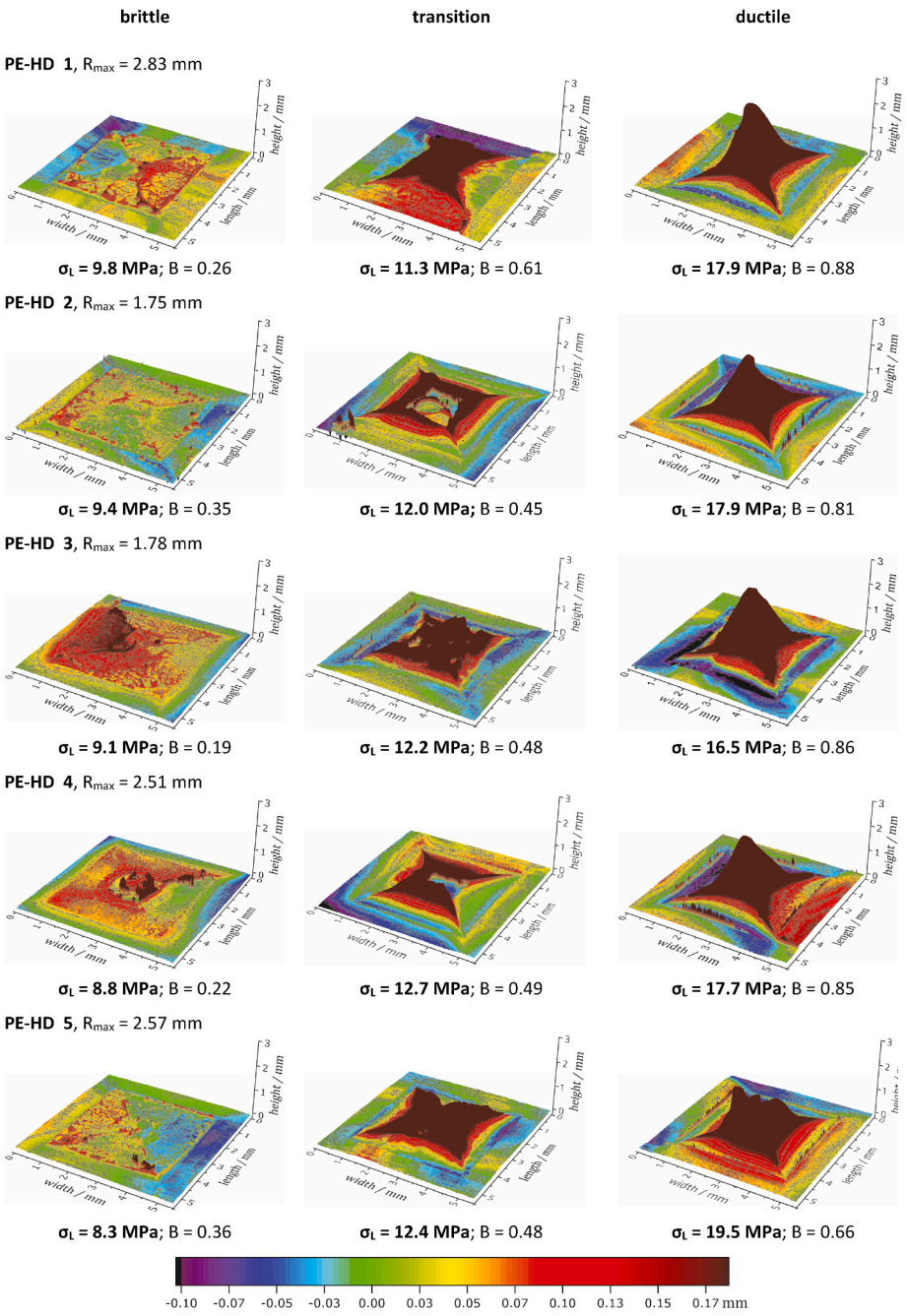

Fig. 7. Exemplary LSM height profile depiction of FNCT fracture surfaces from the brittle, ductile and transition region; PE-HD 1 – PE-HD 5 (group A).

properties of the polymer melt (e.g. molecular mass distribution and chain branches). Furthermore, the ability of polymer chains to disentangle is governed by these properties and might be the main contribution to the occurrence of characteristic fracture surface features. This leads to the correlation of MFR with characteristic FNCT fracture surface features and R_{max}.

In turn, MFR and R_{max} are indicators for the ability of a PE-HD type to show ductile fracture behavior induced by external stress influenced by an environmental liquid: A PE-HD type with a low MFR tends to exhibit more ductile features on an FNCT fracture surface.

It has to be noted that the criterion of brittleness B was only assessed for the FNCT standard test fluid of a 2 wt% aqueous solution of the surfactant Arkopal N 100 (according to ISO 16770). However, B might also be useful in FNCT analysis applying other test fluids. In any case, R_{max} values will have to be redetermined separately for every system of PE-HD type and test fluid. Furthermore, values of B are explicitly only comparable within one system of PE-HD type and test fluid due to the inherent PE-HD type-dependent differences in R_{max}. Therefore, B values obtained for a distinct PE-HD type in a regarded test fluid usually describe very different manifestations of ductile features than those obtained for another PE-HD type in the same test fluid. The criterion of brittleness B might thus be relevant in practical routine testing of common PE-HD types, e.g. in conformity tests of different batches.

5. Conclusion

The occurrence of predominantly brittle fracture behavior is the typical prerequisite to consider FNCT measurements as representative for craze-crack propagation in PE-HD by the ESC damage mechanism. Therefore, a distinct FNCT experiment is only regarded as evaluable

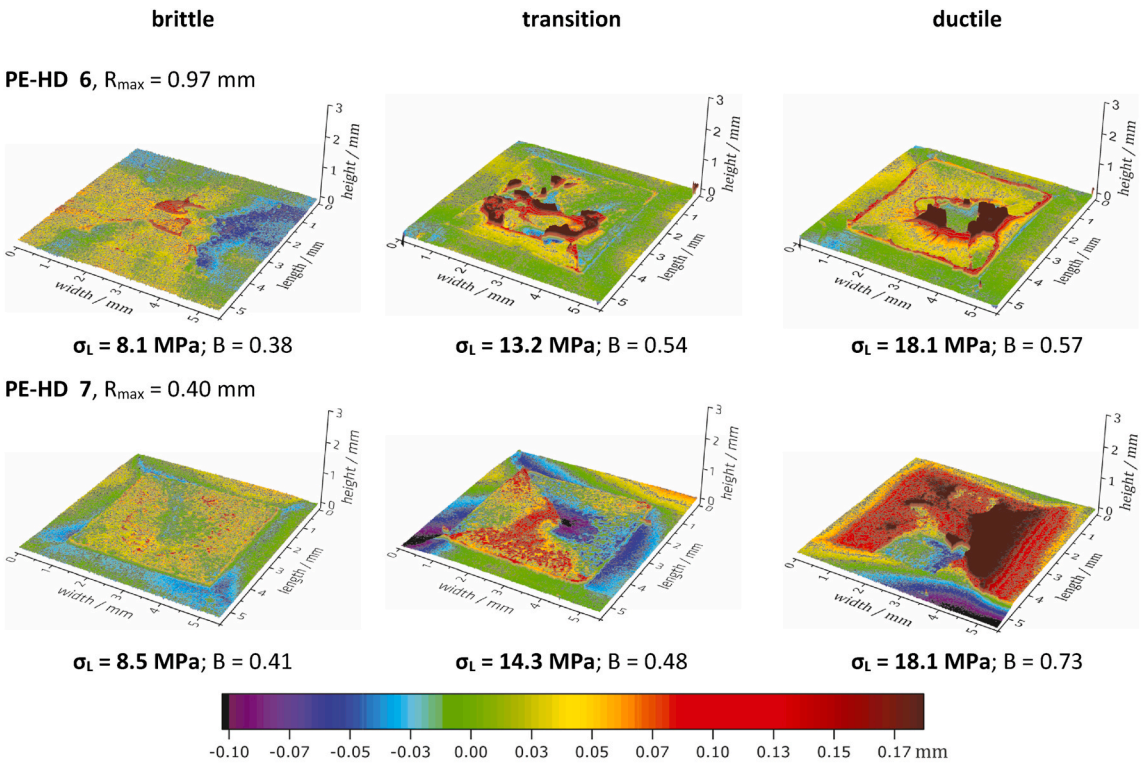

Fig. 8. Exemplary LSM height profile depiction of FNCT fracture surfaces from the brittle, ductile and transition region; PE-HD 6 – PE-HD 7 (group B).

('valid') in practical testing, if a predominantly brittle fracture surface is obtained. To quickly and reliably assess FNCT fracture surfaces with respect to their brittleness, an easy-to-operate phenomenological criterion based on optical LSM height profile data is proposed in this study.

Such a criterion is supposed to be a practical tool in test routines to verify FNCT results according to their significance with respect to ESC. Moreover, it provides a decision aid concerning the evaluability of a distinct FNCT experiment, especially even if the stress-dependent brittle-ductile transition is not easily determinable by classic methods (e.g. by considering the transition point in stress-failure time curves as proposed by the test standard).

The criterion of brittleness B presented in this study is a first proposal for the assessment of fracture surfaces to ensure the evaluability of an FNCT concerning the craze-crack damage mechanism ESC. The development of B is based on empirical FNCT and LSM imaging data obtained for seven PE-HD types tested in the standard surfactant solution of Arkopal N 100. To establish a general validity of B, a larger amount of data for a broader variety of PE-HD types as well as for alternative test conditions (e.g. different test fluids, high temperatures) might be required. However, the enhanced fracture surface analysis developed in this study is a valuable tool for a detailed FNCT evaluation especially in practical routine testing and further methodological improvements.

Declaration of competing interest

The authors declare that they have no known competing financial interests or personal relationships that could have appeared to influence the work reported in this paper.

Acknowledgments

For preparation of FNCT specimens, the help of O. Schwarze and N. Schmidt is especially acknowledged. The support of Department 5 of BAM enabling the participation of N.M. is appreciated.Special thanks to H. Oehler of Fraunhofer LBF for valuable discussions in the framework of the underlying joint research project.

Appendix A. Supplementary data

Supplementary data to this article can be found online at https://doi.org/10.1016/j.polymertesting.2020.107002.

Author statement

The concept of the study was developed by UN, IA and MB and the external funding was acquired by UN and IA. Measurements and analysis were performed by MS with help of NM. Data and results were discussed by MS, UN, NM and MB, figures and visualization were created by MS, NM and MB. The outline of the paper was established by MS and MB who also wrote the text. The final version was read, discussed and agreed upon by all authors.

Funding

The authors are grateful for financial support of AiF, Berlin, Germany [grant number IGF 18606 N] provided by the Federal Ministry of Economic Affairs and Energy based on a resolution of German Bundestag.

Data availability

The raw/processed data required to reproduce these findings cannot be shared at this time as the data also form part of an ongoing study.

References

[1] A.L. Ward, X. Lu, Y. Huang, N. Brown, The mechanism of slow crack growth in polyethylene by an environmental stress cracking agent, Polymer 32 (1991) 2172–2178, https://doi.org/10.1016/0032-3861(91)90043-I.

[2] M. Schilling, U. Niebergall, I. Alig, H. Oehler, D. Lellinger, D. Meinel, M. Böhning, Crack propagation in PE-HD induced by environmental stress cracking (ESC) analyzed by several imaging techniques, Polym. Test. 70 (2018) 544–555, https://doi.org/10.1016/j.polymertesting.2018.08.014.

[3] J.M. Lagarón, J.M. Pastor, B.J. Kip, Role of an active environment of use in an environmental stress crack resistance (ESCR) test in stretched polyethylene: a vibrational spectroscopy and a SEM study, Polymer 40 (1999) 1629–1636, https://doi.org/10.1016/s0032-3861(98)00406-6.
[4] N. Pons, A. Bergeret, J.C. Benezet, L. Ferry, F. Fesquet, An Environmental Stress Cracking (ESC) test to study the ageing of biopolymers and biocomposites, Polym. Test. 30 (2011) 310–317, https://doi.org/10.1016/j.polymertesting.2010.11.015.
[5] J.J. Cheng, M.A. Polak, A. Penlidis, Influence of micromolecular structure on environmental stress cracking resistance of high density polyethylene, Tunn. Undergr. Space Technol. 26 (2011) 582–593, https://doi.org/10.1016/j.tust.2011.02.003.
[6] D.C. Wright, Environmental Stress Cracking of Plastics, Rapra Techology Ltd., Shawbury (UK), 1996, ISBN 1-85957-064-X.
[7] A. Ghanbari-Siahkali, P. Kingshott, D.W. Breiby, L. Arleth, C.K. Kjellander, K. Almdal, Investigating the role of anionic surfactant and polymer morphology on the environmental stress cracking (ESC) of high-density polyethylene, Polym. Degrad. Stabil. 89 (2005) 442–453, https://doi.org/10.1016/j.polymdegradstab.2005.01.023.
[8] M. Fleissner, Experience with a full notch creep test in determining the stress crack performance of polyethylenes, Polym. Eng. Sci. 38 (1998) 330–340, https://doi.org/10.1002/pen.10194.
[9] R. Ayyer, A. Hiltner, E. Baer, Effect of an environmental stress cracking agent on the mechanism of fatigue and creep in polyethylene, J. Mater. Sci. 43 (2008) 6238–6253, https://doi.org/10.1007/s10853-008-2926-1.
[10] A. Lustiger, R.L. Markham, Importance of tie molecules in preventing polyethylene fracture under long-term loading conditions, Polymer 24 (1983) 1647–1654, https://doi.org/10.1016/0032-3861(83)90187-8.
[11] M.K.V. Chan, J.G. Williams, Slow stable crack growth in high density polyethylenes, Polymer 24 (1983) 234–244, https://doi.org/10.1016/0032-3861(83)90139-8.
[12] I.M. Ward, J. Sweeney, Mechanical Properties of Solid Polymers, third ed., John Wiley & Sons Ltd., Chichester, 2013, ISBN 978-1-4443-1950-7 https://doi.org/10.1002/9781119967125.
[13] R.A.C. Deblieck, D.J.M. van Beek, K. Remerie, I.M. Ward, Failure mechanisms in polyolefines: the role of crazing, shear yielding and the entanglement network, Polymer 52 (2011) 2979–2990, https://doi.org/10.1016/j.polymer.2011.03.055.
[14] N. Brown, X. Lu, A fundamental theory for slow crack growth in polyethylene, Polymer 36 (1995) 543–548, https://doi.org/10.1016/0032-3861(95)91563-M.
[15] R. Qian, X. Lu, N. Brown, Investigating the existence of a threshold stress intensity for slow crack-growth in high-density polyethylene, J. Mater. Sci. 24 (1989) 2467–2472, https://doi.org/10.1007/Bf01174513.
[16] X.C. Lu, Z.Q. Zhou, N. Brown, A sensitive mechanical test for slow crack growth in polyethylene, Polym. Eng. Sci. 37 (1997) 1896–1900, https://doi.org/10.1002/pen.11839.
[17] M. Schilling, Environmental Stress Cracking (ESC) and Slow Crack Growth (SCG) of PE-HD Induced by External Fluids, PhD Thesis, Technical University Darmstadt, 2020, https://doi.org/10.25534/tuprints-00011544.
[18] M. Schilling, U. Niebergall, M. Böhning, Full notch creep test (FNCT) of PE-HD – characterization and differentiation of brittle and ductile fracture behavior during environmental stress cracking (ESC), Polym. Test. 64 (2017) 156–166, https://doi.org/10.1016/j.polymertesting.2017.09.043.
[19] ISO 16770, Plastics - Determination of Environmental Stress Cracking (ESC) of Polyethylene - Full-Notch Creep Test (FNCT), 2004.
[20] X.C. Lu, X.Q. Wang, N. Brown, Slow fracture in a homopolymer and copolymer of polyethylene, J. Mater. Sci. 23 (1988) 643–648, https://doi.org/10.1007/Bf01174699.
[21] DIN DVS 2203-4, addendum 2, Testing of Welded Joints of Thermoplastic Panels and Pipes - Tensile Creep Test for Resistance to Slow Crack Growth in the Full Notch Creep Test (FNCT), 2016 (DVS 2203-4-2:2016); German version.
[22] DIN EN ISO 293, Plastics - Compression Moulding of Test Specimens of Thermoplastic Materials, 2005 (ISO 293:2004); German version.
[23] DIN EN ISO 17855-2, Plastics - Polyethylene (PE) Moulding and Extrusion Materials - Part 2: Preparation of Test Specimens and Determination of Properties, 2016 (ISO 17855-2:2016); German version.
[24] DIN EN ISO 13274, Packaging - Transport Packaging for Dangerous Goods - Plastics Compatibility Testing for Packaging and IBCs, German version, 2014.
[25] DIN EN ISO 11542-2, Plastics - Ultra-high-molecular-weight Polyethylene (PE-UHMW) Moulding and Extrusion Materials - Part 2: Preparation of Test Specimens and Determination of Properties, 2010 (German version).
[26] M. Schilling, M. Böhning, H. Oehler, I. Alig, U. Niebergall, Environmental stress cracking of polyethylene high density (PE-HD) induced by liquid media - validation and verification of the full-notch creep test (FNCT), Mat. Sci. Eng. Tec. 48 (2017) 846–854, https://doi.org/10.1002/mawe.201700065.
[27] R.J. Renka, A.K. Cline, A triangle-based c-1 interpolation method, Rocky Mt, J. Mat. 14 (1984) 223–237, https://doi.org/10.1216/Rmj-1984-14-1-223.
[28] ISO 4287:2010, Geometrical Product Specifications (GPS) – Surface Texture: Profile Method – Terms, Definitions and Surface Texture Parameters, German version, 2010.
[29] C. Grein, K. Bernreitner, A. Hauer, M. Gahleitner, W. Neissl, Impact modified isotatic polypropylene with controlled rubber intrinsic viscosities: some new aspects about morphology and fracture, J. Appl. Polym. Sci. 87 (2003) 1702–1712, https://doi.org/10.1002/app.11696.